A closer look at the indications of q-generalized Central Limit Theorem behavior in quasi-stationary states of the HMF model

Alessandro Pluchino

Dipartimento di Fisica e Astronomia, Universitá di Catania, and INFN sezione di Catania, Via S. Sofia 64, I-95123 Catania, Italy

Andrea Rapisarda

Dipartimento di Fisica e Astronomia, Universitá di Catania, and INFN sezione di Catania, Via S. Sofia 64, I-95123 Catania, Italy

Constantino Tsallis

Centro Brasileiro de Pesquisas Fisicas, Rua Xavier Sigaud 150, 22290-180 Rio de Janeiro-RJ, Brazil
and
Santa Fe Institute, 1399 Hyde Park Road, NM 87501, USA

Abstract

We give a closer look at the Central Limit Theorem (CLT) behavior in quasi-stationary states of the Hamiltonian Mean Field model, a paradigmatic one for long-range-interacting classical many-body systems. We present new calculations which show that, following their time evolution, we can observe and classify three kinds of long-standing quasi-stationary states (QSS) with different correlations. The frequency of occurrence of each class depends on the size of the system. The different microsocopic nature of the QSS leads to different dynamical correlations and therefore to different results for the observed CLT behavior.

Key words: Metastability in Hamiltonian dynamics; Long-range interactions; Central Limit Theorem behavior; Nonextensive statistical mechanics.

Email addresses: alessandro.pluchino@ct.infn.it (Alessandro Pluchino), andrea.rapisarda@ct.infn.it (Andrea Rapisarda), tsallis@cbpf.br (Constantino Tsallis).

1 Introduction

Very recently there has been a lot of interest in generalizations of the Central Limit Theorem (CLT) [1,2,3] and on their possible (strict or numerically approximate) application to systems with long range correlations [4,5], at the edge-of-chaos [6], nonlinear dynamical systems the maximal Lyapunov exponent of which is either exactly zero or tends to vanish in the thermodynamic limit (increasingly large systems) [7], hindering this way mixing and thus the application of standard statistical mechanics. A possible application of nonextensive statistical mechanics [8,9] has been advocated in these cases. Along this line we discuss in the present paper a detailed study of a paradigmatic *toy model* for long-range interacting Hamiltonian systems [10,11,12,13,14,15,16], i.e. the Hamiltonian Mean Field (HMF) model which has been intensively studied in the last years. In a recent article [17], we presented molecular dynamics numerical results for the HMF model showing three kinds of quasi-stationary states (QSS) starting from the same water-bag initial condition with unitary magnetization ($M_0 = 1$). In the following we present how the applicability of the standard or q-generalized CLT is influenced by the different microscopic dynamics observed in the three classes of QSS. In general, averaging over the threee classes can be misleading. Indeed, the frequency of appearence of each of these classes depends on the size of the system under investigation, and there is no clear evidence that a predominant class exists.

2 Quasi-stationary behavior in the HMF model

The HMF model consists of N fully-coupled classical inertial XY spins (rotors) $\vec{s_i} = (cos\ \theta_i, sin\ \theta_i)$, $i = 1, ..., N$, with unitary module and mass [10]. One can also think of these spins can as rotating particles on the unit circle. The Hamiltonian is given by

$$H = \sum_{i=1}^{N} \frac{{p_i}^2}{2} + \frac{1}{2N} \sum_{i,j=1}^{N} [1 - cos(\theta_i - \theta_j)] \quad , \tag{1}$$

where θ_i ($0 < \theta_i \leq 2\pi$) is the angle and p_i the conjugate variable representing the rotational velocity of spin i.
At equilibrium the model can be solved exactly and the solution predicts a second order phase transition from a high temperature paramagnetic phase to a low temperature ferromagnetic one [10]. The transition occurs at the critical temperature $T_c = 0.5$ which corresponds to a critical energy per particle $U_c = E_c/N = 0.75$. The order parameter is the modulus of the *average mag-*

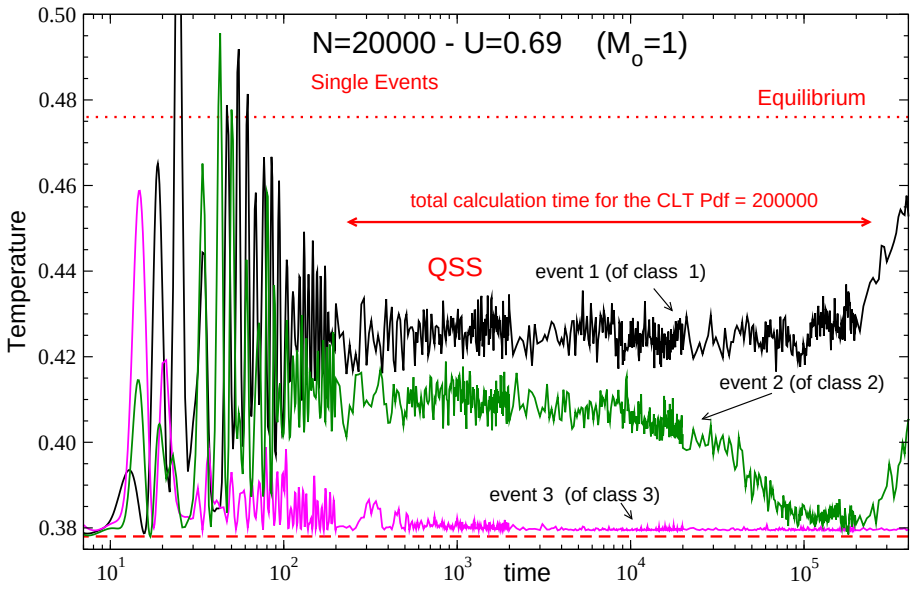

Fig. 1. Time evolution of the temperature (calculated as twice the average kinetic energy per particle) for three single events representative of the three different classes observed at $U = 0.69$ for initial magnetization $M_0 = 1$. The size of the system is $N = 20000$.

netization per spin defined aa $M = (1/N)|\sum_{i=1}^{N} \vec{s_i}|$. Above T_c, the spins are homogeneously distributed on the circle so that $M \sim 0$, while below T_c, most spins are aligned, i.e. rotors are trapped in a single cluster, and $M \neq 0$. The out-of equilibrium dynamics of the model presents very interesting dynamical anomalies. For energy densities $U \in [0.5, 0.75]$, special classes of initial conditions such as those called *water-bag*, characterized by an initial magnetization $0 \leq M_0 \leq 1$ and uniform distribution of the momenta, drive the system, after a violent relaxation, towards metastable QSS. The latter slowly decay towards equilibrium with a lifetime which diverges like a power of the system size N [10]. Along the QSS regime, in the microcanonical ensemble, the dynamics exhibits a glassy behavior, hierarchical structures, velocity correlations, aging, vanishing Lyapunov exponents, etc., and the statistical description of the QSS is strongly dependent on the initial conditions [11,12,13]. However, even for the same type of initial conditions, we have observed different dynamical behaviors [17]. In particular we have found three typical classes of events, as illustrated in Fig. 1. Here we plot the temperature of the system (defined as twice the average kinetic energy per particle) versus time. We focused on a system with size $N = 20000$, the energy per particle being $U = 0.69$, for which anomalies are more evident. Initial conditions were chosen to be of the water-bag kind, with initial magnetization equal to unity ($M_0 = 1$). For details about the accuracy of the calculations and the integration algorithm adopted see Ref.[12]. Only single events are plotted in Fig. 1, each one representative of a given class. One immediately realizes that there are two extreme events (which we indicated with 1 and 3) and an intermediate one (indicated as 2)

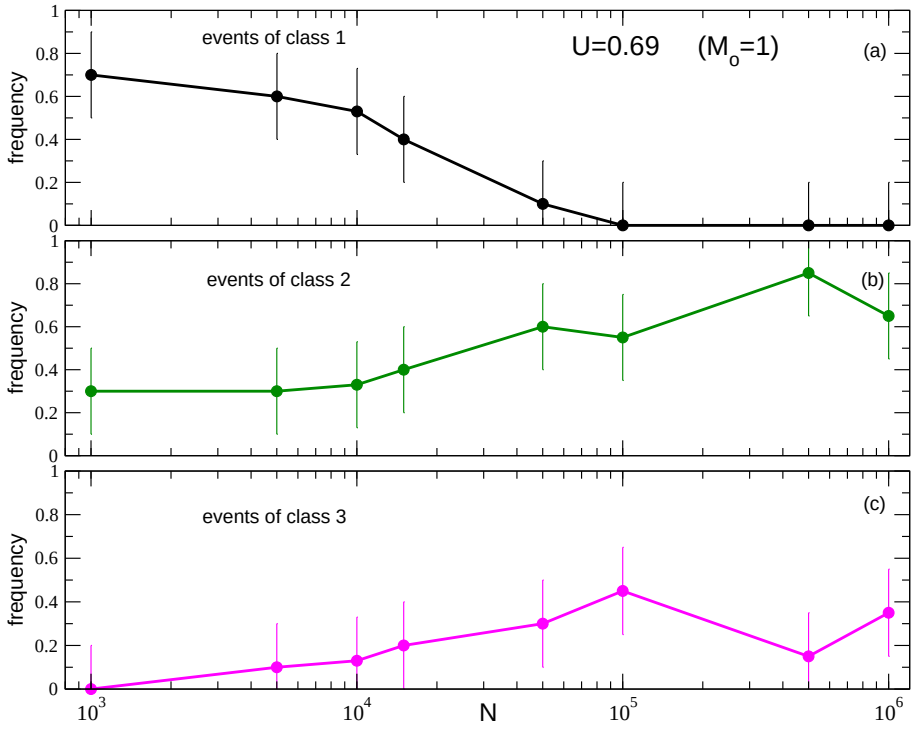

Fig. 2. Relative frequency of occurrence for the three classes of events shown in Fig. 1 as a function of N. A total of $m = 20$ realizations for each N was considered. We report also an uncertainty equal to $\pm\Delta = 1/\sqrt{m}$. The three curves add up to unity.

which stays close to event 1 at the beginning, but collapses towards the plateau of the event 3 after some time. The relative frequency of occurrence of these three classes of events is illustrated in Fig. 2 as a function of the size N of the system. A total of 20 realizations for each N was considered. It is important to note that the event of class 3 shown in Fig. 1, and all the events of class 3 in general, are very similar to the QSS obtained for initial conditions with zero initial magnetization ($M_0 = 0$), which are almost homogeneous and have very small correlations [12]. In this case a Lynden-Bell kind of approach, or one based on the Vlasov equation has been applied [15]. Therefore, due to the different nature of these QSS, which have in general different microscopic correlations, one could expect a different result for the central limit theorem behavior shown in Refs. [16,18,19].

3 Discussion of numerical results for the CLT

In this section, following the prescription of the CLT and the procedure adopted in Refs. [16,18,19], we construct probability density functions (Pdf) of quantities expressed as a finite sum of stochastic variables and we select these variables along the deterministics time evolutions of the N rotors. More

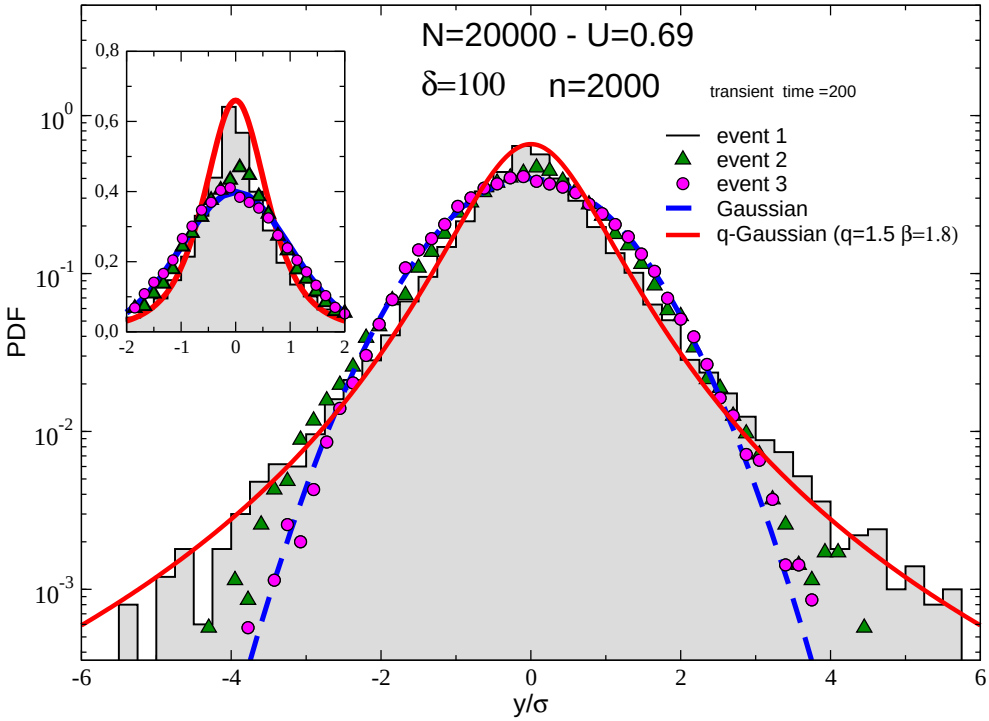

Fig. 3. We present for each class of the QSS found, the different central limit theorem behavior observed. A Gaussian (dashed curve) with unitary variance and a q-Gaussian $p(x) = Ae_q(-\beta x^2)$ with $A = 0.66$ $q = 1.5$ and $\beta = 1.8$ (full curve) are also reported for comparison. In the inset a magnification of the central part in linear scale is plotted. See text for further details.

formally, we study the Pdf of the quantity y defined as

$$y_i = \frac{1}{\sqrt{n}} \sum_{k=1}^{n} p_i(k) \quad for \quad i = 1, 2, ..., N \quad , \tag{2}$$

where $p_i(k)$, with $k = 1, 2, ..., n$, are the rotational velocities of the ith-rotor taken at fixed intervals of time δ along the same trajectory obtained integrating the HMF equations of motions. The product $\delta \times n$ gives the total simulation time over which the sum of Eq. (2) is calculated. As stressed in Ref. [18], the variables y's are also proportional to the *time average* of the velocities along the single rotor trajectories (in fact the $1/\sqrt{n}$ scaling is not necessary, and has been adopted just to conform to usage).

In Fig. 3 we show how the shape of the y's Pdf is affected by the existence of different classes of events in the QSS of the HMF model. We consider the same system of the previous section with $N = 20000$, $U = 0.69$ and $M_0 = 1$ initial conditions. Then we plot the Pdfs corresponding to the three different events shown in Fig. 1, the sum (2) being calculated over all the QSS extension with $\delta = 100$ and $n = 2000$ (for a total time of 200000 steps, after a transient of 200, see orizontal arrow in Fig.1). All the curves were normalized

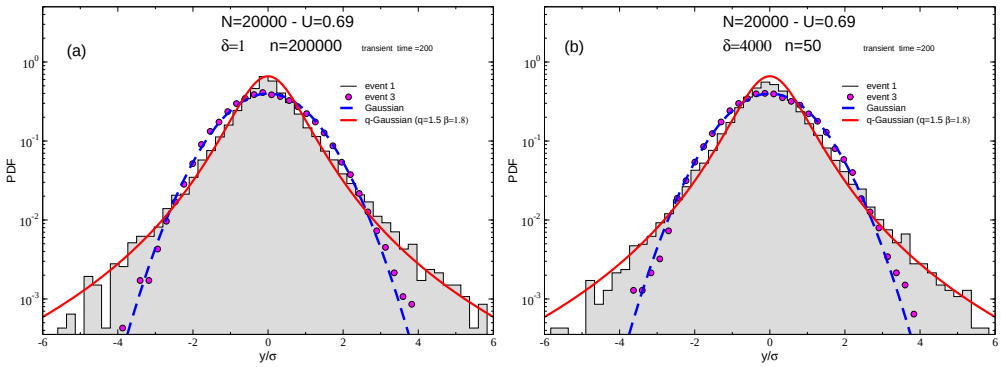

Fig. 4. CLT Pdfs for the same events 1 and 3 of Fig. 3, but with different values of δ and n. A Gaussian (dashed curve) with unitary variance and a q-Gaussian with $A = 0.66$, $q = 1.5$ and $\beta = 1.8$ (full curve) are also reported for comparison.

to their standard deviations in order to compare them (notice that, as done in [16], in the Eq. (2) we do not subtract an average value calculated over the trajectory and all rotors as in [18,19] since it is not important due to this kind of normalization). In case of no global correlations, as one would expect at equilibrium, the standard CLT holds and the resulting Pdf should be a Gaussian (reported as dashed line for comparison). This fact has been verified for the equilibrium case in [18]. Actually this is also what happens for the event 3 (full circles) and it is most probably due to its similarity with the homogeneous QSS recalled in the previous section. On the other hand, if one considers the event 1 (gray histogram), strong deviations from the Gaussian behavior appears, meaning that global correlations become important. In this case a very good fit is obtained with a q-Gaussian defined as

$$p(x) = A\, e_q(-\beta x^2) = \frac{A}{[1 + (q-1)\beta x^2]^{1/(q-1)}}\,, \tag{3}$$

where $A(q, \beta)$ is a normalizing constant, which coincides in fact with $p(0)$. An excellent fitting corresponds to $p(y/\sigma) = 0.66\, e_{1.5}^{-1.8\,(y/\sigma)^2}$ (full line), a result very similar to those discussed in Refs. [18,19]. Finally, the Pdf of event 2 (full triangles) lies between the previous two, being (within the time interval that has been observed) neither Gaussian nor q-Gaussian but a sort of mixture of them, due to the presence of a double QSS plateau in the temperature evolution of this event. This new scenario, where both Gaussian and q-Gaussian attractors appear in the QSS of a given system, implies that, if an average of the y's is performed on many realizations, the particular mixture of the three kinds of events discussed here will affect the resulting Pdf, in particular for sizes of the system greater than $N = 10000$ (i.e. when the relative frequency of events of class 3 becomes important). In this respect, such a scenario also qualifies the context within which the results presented in Refs. [18,19] are to be considered, which is thus not general, especially for large system sizes.

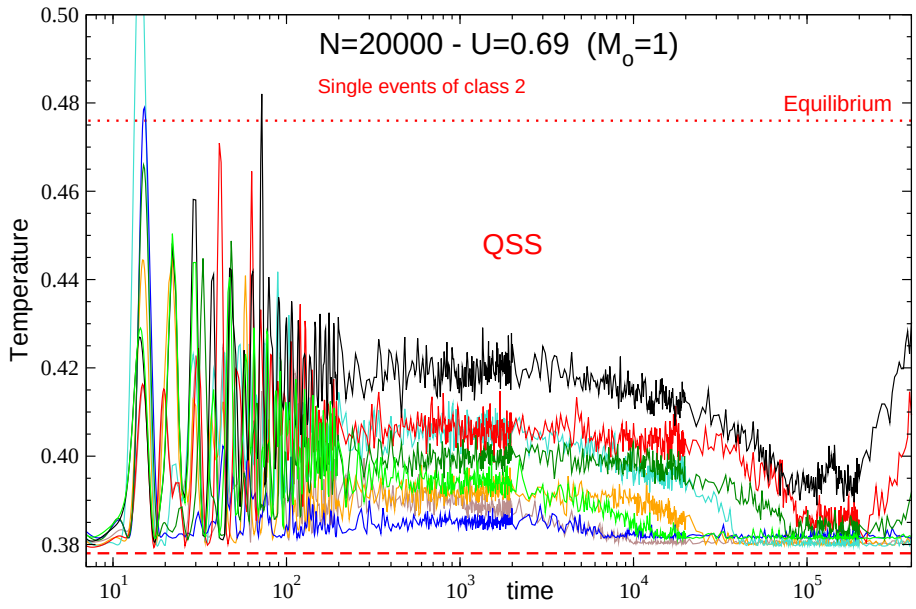

Fig. 5. Different events of class 2 are plotted for the case N=20000. A large variability is observed for this class, at variance with the other two.

As a further remark, in Fig. 4 we test the robustness of the behavior observed in Fig. 3 for events 1 and 3. We repeated the calculations on the same events of Fig. 3, but with a different time interval δ. In the figure we report the cases $\delta = 1$ (a) and $\delta = 4000$ (b). One can see that changing δ and n in the calculation of the y's unaffects the Pdf's shape corresponding to those events, providing that the total simulation time (i.e. the product $\delta \times n$) remains unchanged. In this figure, the same Gaussian and q-Gaussian curves of Fig. 3 are plotted again for comparison. It is important to notice that, for the case $N = 20000$ discussed in this article, we did not study in detail the behavior of the CLT for the events of class 2. In this case one could probably distinguish a first time evolution, closer to events of class 1, from a final time evolution closer to events of class 3. In the present case, however, the first part of the plateau is too short to allow the investigation of the CLT behavior. The latter can probably be done for systems of larger sizes: we leave this study for the future. However, there is another difficulty which is intrinsic with the events of this class. In fact they exhibit a general strong variability as shown in Fig. 5, where we plot the temperature time evolution for several different events of class 2 for the case $N = 20000$. Although the qualitative behavior with a double plateau is the same, the temperature of the initial plateau can vary. In this respect a more detailed investigation is in progress.

Before concluding, we would like to illustrate that the CLT behavior observed for the events of class 3 for $M_0 = 1$ initial conditions is equivalent to that observed for any typical event with initial conditions $M_0 = 0$. In Fig. 6 we plot the CLT behavior for $M_0 = 0$ in comparison with the case $M_0 = 1$ for class 1 events, previously reported in Fig. 3. The Gaussian Pdf obtained for

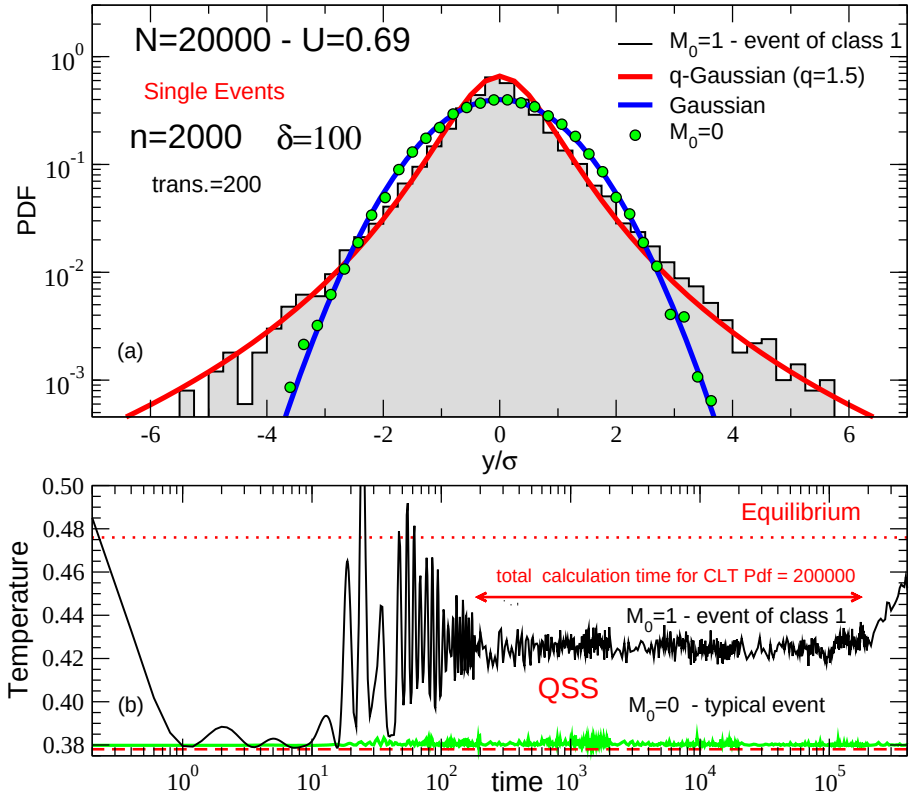

Fig. 6. (a) Comparison of the CLT behavior for the case $U = 0.69$ initial magnetization $M_0 = 1$ (class 1) vs $M_0 = 0$. The size of the system is $N = 20000$. A Gaussian (dashed curve) with unitary variance and a q-Gaussian with $A = 0.66$, $q = 1.5$ and $\beta = 1.8$ (full curve) are also reported for comparison. (b) Temperature time evolutions of the same events shown in panel (a).

the case $M_0 = 0$ is comparable with what obtained in Fig. 3 for the events of class 3.

In Ref. [18], we showed a clear inequivalence between time averages and ensemble averages. In Fig. 7, we show that this inequivalence persists also for different initial conditions and classes. The ensemble averages of velocities are considered at time $t = 1000$ inside the QSS over 10 events. The Pdfs plotted in panels (a) and (b) are to be compared with the time averages curves shown in panel (a) of Fig. 6, while those plotted in panels (c) and (d) are to be compared with the time averages curves of events 1 and 3 of Fig. 3. A Gaussian (dashed curve) with unitary variance and a q-Gaussian with $A = 0.66$, $q = 1.5$ and $\beta = 1.8$ (full curve) are also reported for comparison. It is clear that the curves in Fig. 7 are neither Gaussian nor q-Gaussians.

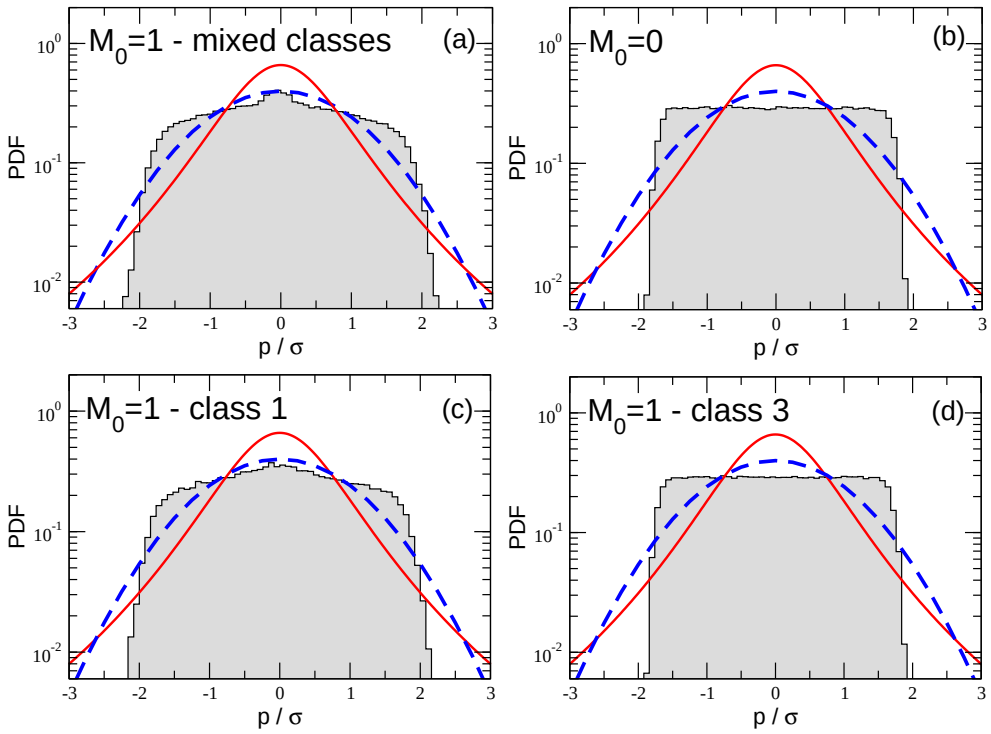

Fig. 7. Ensemble averages of velocities for $N = 20000$, $U = 0.69$ taken at time $t = 1000$ in the QSS regime for different initial conditions and classes of events. The average was done over 10 events. A Gaussian (dashed curve) with unitary variance and a q-Gaussian with $A = 0.66$, $q = 1.5$ and $\beta = 1.8$ (full curve) are also reported for comparison. See text for further details.

4 Conclusions

On the basis of the new calculations presented here, one should distinguish among different classes of QSS for a given size of the HMF system. Our tests do confirm that correlations can be different for different dynamical realizations of the same system, starting from the same class of initial conditions, and therefore also the Central Limit Theorem behavior can change. According to the class considered we can have a Gaussian Pdf, a q-Gaussian one or a mixture between the two. In this respect, the presence of a q-Gaussian curve confirms the results previously published about the indications for a generalized CLT in long-range Hamiltonian systems when ergodicity is broken and correlations are strong enough. The present results, where we verify that the time evolution of the system is quite sensitive to the specific initial conditions, reminds what occurs in other anomalous systems, like the Hydrogen atom as studied recently in Refs. [20,21]. We have checked also that inequivalence between time averages and ensemble averages continues to hold within the different classes for $M_0 = 1$ and for $M_0 = 0$ initial conditions. Finally, although it is true that the frequency of occurrence of events of class 1 and 2 for very large sizes, and in particular the attractor for the events of class

2, remain to be investigated with more accuracy (calculations with better statistics are in progress) before advancing definitive conclusions, from these simulations one could conjecture that the events of class 1 tend to disappear in the thermodynamic limit. However, even if this was the case, their probability of occurrence (as well as the probability of occurrence of the first metastable plateau of events of class 2) can be significantly different from zero for large but finite systems and therefore the applicability of q-statistics in metastable states of real complex systems remains a valid and interesting possibility.

Acknowledgments

The present calculations were done within the Trigrid project and we thank M. Iacono Manno for technical help. A.P. and A.R. acknowledge financial support from the PRIN05-MIUR project "Dynamics and Thermodynamics of Systems with Long-Range Interactions". C.T. acknowledges partial financial support from the Brazilian Agencies CNPq and Faperj.

References

[1] C. Tsallis, Milan J. Math. **73** (2005) 145, and references therein.

[2] S. Umarov, C. Tsallis and S. Steinberg, cond-mat/0603593 (2006;) S. Umarov and C. Tsallis, cond-mat/0703553 (2007); S. Umarov and C. Tsallis, American Institute of Physics Conference Proceedings **965** (2007) 34.

[3] A. Rebenshtok and E. Barkai, Phys. Rev. Lett. **99** (2007) 210601.

[4] L.G. Moyano, C. Tsallis and M. Gell-Mann, Europhys. Lett. **73** (2006) 813; J.A. Marsh, M.A. Fuentes, L.G. Moyano and C. Tsallis, Physica A **372** (2006) 183; C. Tsallis and S.M.D. Queiros, American Institute of Physics Conference Proceedings **965** (2007) 8; S.M.D. Queiros and C. Tsallis, American Institute of Physics Conference Proceedings **965** (2007) 21.

[5] H.J. Hilhorst and G. Schehr, J. Stat. Mech. (2007) P06003.

[6] U. Tirnakli, C. Beck and C. Tsallis, Phys. Rev. E **75**, 040106(R) (2007).

[7] C. Anteneodo and C. Tsallis, Phys. Rev. Lett. **80** (1998) 5313.

[8] C. Tsallis, *J. Stat. Phys.* **52** (1988) 479; M. Gell-Mann and C. Tsallis, eds., *Nonextensive Entropy - Interdisciplinary Applications* (Oxford University Press, New York, 2004); J.P. Boon and C. Tsallis, eds., Europhys. News **36** (6) (2005).

[9] C. Tsallis, M. Gell-Mann and Y. Sato, Proc. Natl. Acad. Sci. (USA) **102** (2005) 15377 and references therein.

[10] T. Dauxois, V. Latora, A. Rapisarda, S. Ruffo and A. Torcini, in *Dynamics and Thermodynamics of Systems with Long Range Interactions*, T. Dauxois, S. Ruffo, E. Arimondo and M. Wilkens, eds., Lecture Notes in Physics **602** (Springer, Heidelberg, 2002) p. 458; A. Pluchino, V. Latora and A. Rapisarda, Continuum Mechanics and Thermodynamics, **16** (2004) 245; P.H. Chavanis, J. Vatteville and F. Bouchet, Eur. Phys. J. **B 46** (2005) 61.

[11] V. Latora, A. Rapisarda and C. Tsallis, Physica A **305** (2002) 129; B.J.C. Cabral and C. Tsallis, Phys. Rev. E **66** (2002) 065101(R).

[12] A. Pluchino, V. Latora and A. Rapisarda, Physica D **193** (2004) 315; A. Rapisarda and A. Pluchino, Europhysics News **36** (2005) 202; A. Pluchino and A. Rapisarda, Progr. Theor. Phys. Supplement **162** (2006) 18; A. Pluchino, V. Latora and A. Rapisarda, Physica A **370** (2006) 573.

[13] P.H. Chavanis, Eur. J. Phys. **B 53** (2006) 487.

[14] F. Baldovin and E. Orlandini, Phys. Rev. Lett. **96** (2006) 240602 and Phys. Rev. Lett. **97** (2006) 100601.

[15] A. Antoniazzi, F. Califano, D. Fanelli, S. Ruffo Phys. Rev. Lett 98 (2007) 150602; A. Antoniazzi, D. Fanelli, J. Barré, P.H. Chavanis, T. Dauxois and S. Ruffo, Phys. Rev. E **75**, 011112 (2007).

[16] C. Tsallis, A. Rapisarda, A. Pluchino and E. Borges, Physica A **381** (2007) 143.

[17] A. Pluchino and A. Rapisarda, American Institute of Physics Conference Proceedings **965** (2007) 129.

[18] A. Pluchino, A. Rapisarda and C. Tsallis, Europhys. Lett. **80** (2007) 26002

[19] A. Pluchino, A. Rapisarda, proceedings of the International SPIE conference on Complex Systems, Canberra 5-7 December (2007), arxiv:/0712.2539, in press.

[20] N.M. Oliveira-Neto, E.M.F. Curado, F.D. Nobre and M.A. Rego-Monteiro, Physica A **374** (2007) 251.

[21] N.M. Oliveira-Neto, E.M.F. Curado, F.D. Nobre et al, J. Phys. B **40** (2007) 1975.